

# Modelling of Polarization-Dependent Loss in Plasmonic Nanowire Waveguides

Tiberiu Rosenzveig · Petur G. Hermannsson · Kristjan Leosson

Received: 24 March 2009 / Accepted: 22 December 2009 / Published online: 16 January 2010  
© Springer Science+Business Media, LLC 2010

**Abstract** We have investigated the potential of using gold nanowires embedded in a dielectric cladding environment as polarization-independent long-range surface plasmon polariton waveguides at telecom wavelengths. We performed finite-element analysis on various symmetric and close-to-symmetric cross-sectional geometries and evaluated the effects of cladding thickness on the propagation and coupling loss. The calculations confirm that fabrication of polarization-independent waveguides with reasonable tolerances is feasible and that straight-waveguide insertion losses around 1.5 dB for short (0.5 mm) devices can be realized when coupling to and from conventional dielectric waveguide geometries.

**Keywords** Surface plasmons · Nanowires · Integrated optics

The field of surface plasmon–polariton (SPP) optics has attracted considerable interest recently. Passive and active devices based on surface plasmons have been proposed to complement conventional dielectric optical circuits [1]. There are mainly two potential advantages that devices based on SPPs can offer over traditional dielectric technologies: firstly, since the electromagnetic mode is strongly bound to the interface between the dielectric and the metal, a much higher degree of confinement is possible than with dielectric waveguides. On one hand, this allows for very compact devices to be designed and fabricated as light can be compressed to below the diffraction limit and, on the other hand, very high field intensities can be realized in relatively small volumes. Secondly, the bound electromagnetic wave is very sensitive to changes to the refractive

index of the surrounding medium, making SPPs a prime candidate for sensing applications [2].

SPP circuits do, however, have several drawbacks when compared with traditional dielectric waveguides. The plasmon–polaritons propagating at the interface between a metal and a dielectric exhibit a high propagation loss due to the damping effect of the metal. This problem can be somewhat mitigated by using a thin film of metal (with thickness on the order of 10 nm) sandwiched between dielectric layers with equal refractive index [3–6]. In this case, the SPPs propagating at the upper and lower interface of the metal film couple and form a long-range surface plasmon polariton (LRSPP) supermode that is weakly bound to the metal film, thus reducing the losses. However, devices based on such waveguides only support modes with the electric field polarized perpendicular to the metal strip which is a strong disadvantage in interfacing with conventional fiber-optics. Berini suggested substituting the metal strip with a metallic nanowire with a symmetric square cross-section to solve the polarization problem [7] and propagation of orthogonal linear polarizations in such wires was recently confirmed experimentally [8]. Unlike the metallic strip, a wire with a square cross-section can support long-range supermodes with the electric field polarized predominantly along the  $x$  or  $y$  directions (denoted by Jung et al. [9] as  $E^{(1,0)}$  and  $E^{(0,1)}$ , respectively). These supermodes are formed by specific superpositions of four corner-plasmon–polariton modes that propagate along the edges of the wire.

In this paper, we present simulations of propagation loss (due to metal absorption) and coupling loss (to standard single-mode fibers) at 1,550 nm wavelength for straight nanowire waveguides. The waveguides consist of gold wires embedded in a polymer cladding. We also calculate the effects of slight deviations from the symmetrical square

T. Rosenzveig (✉) · P. G. Hermannsson · K. Leosson  
Department of Physics, Science Institute, University of Iceland,  
Dunhagi 3,  
IS-107 Reykjavik, Iceland  
e-mail: jptibirosen@raunvis.hi.is

cross-section (rectangular and trapezoidal waveguides) on the polarization-dependent loss. Previous simulations of plasmonic nanowire waveguides in the literature have been concerned with modeling wires in an infinite cladding environment [9]. Here, we consider the effects of a finite cladding thickness on the loss figures and show how a finite cladding thickness can substantially affect the propagation and coupling loss. A suitable cladding geometry can thus be used to reduce the total insertion loss of short nanowire waveguide devices.

We performed finite-element analysis on plasmonic waveguides consisting of gold nanowires embedded in a polymer cladding. Commercially available finite-element software, COMSOL Multiphysics (RF module) was used for modeling. The modelled system consisted of a gold nanowire, characterized by a complex refractive index  $\tilde{n} = 0.52 + 10.7i$  at 1,550 nm wavelength [10] surrounded by dielectric with  $n = 1.535$  (similar to, e.g., [4]), bounded by air on all sides as shown in the inset of Fig. 1. For simplicity, we did not take into account the presence of a substrate. For thin cladding layers, radiation will leak into a high-index substrate (e.g., silicon) but this can be avoided by using an intermediate lower-index dielectric layer between the cladding and the substrate.

We first investigated nanowires with square cross-section with different side lengths. To avoid unrealistically

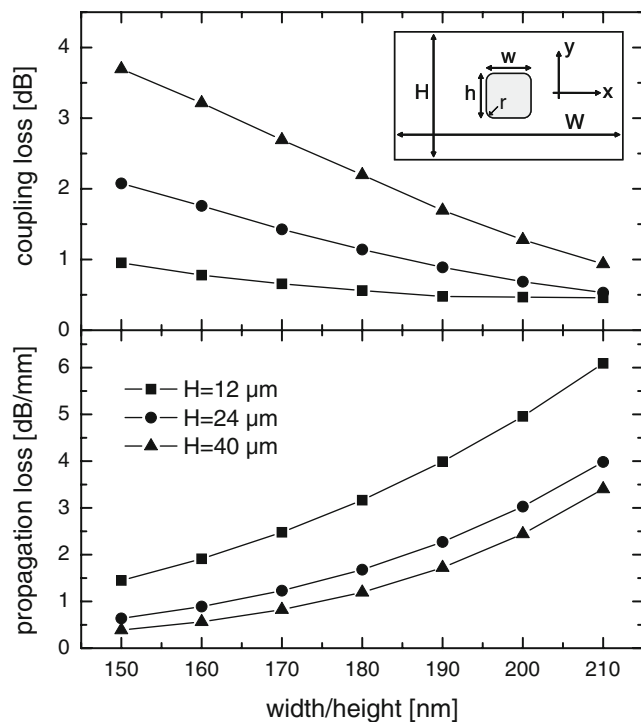


**Fig. 1** Coupling loss and propagation loss in symmetric nanowire waveguides. Calculations for three different cladding thicknesses are shown. Results are shown for the long-range mode with the electric field polarized in the  $y$ -direction, as indicated in the figure

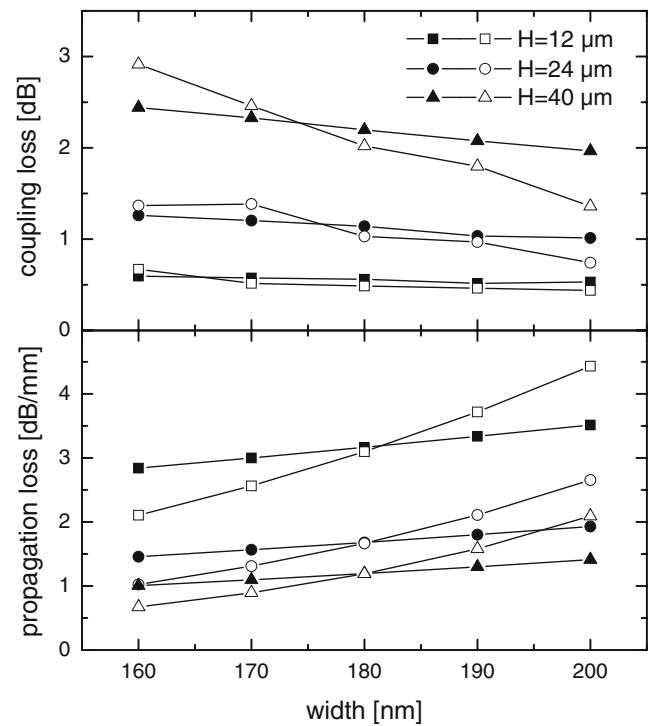


**Fig. 2** Propagation loss and coupling loss in asymmetric nanowire waveguides for the  $y$ -polarized  $E^{(0,1)}$  mode (closed symbols) and the  $x$ -polarized  $E^{(1,0)}$  mode (open symbols). The height of the wires is fixed at  $h = 180$  nm

sharp corners, the squares were rounded with a radius of 5 nm. The literature suggests [9] that a modest rounding of the corners has a minimal effect on the results of the finite-element calculations. Propagation loss was determined from the calculated effective refractive index of the linearly polarized supermodes, whereas coupling loss was obtained from the 2-D overlap integral between the LRSPP mode field and the field from a standard single-mode optical fiber

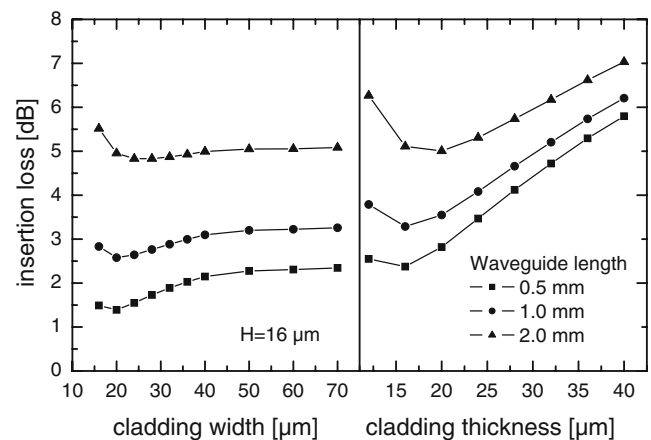


**Fig. 3** Total insertion loss for different lengths of symmetric nanowire waveguides ( $180 \times 180$  nm) when the extent of the dielectric cladding layer is limited vertically (right panel) and both vertically and horizontally (left panel)

(taken as Gaussian, with a mode-field diameter of 10.5  $\mu\text{m}$ ). It should be noted that the maximum overlap between the fiber mode and the LRSPP mode occurs where the 1/e mode width measure used in [9] is much smaller than the 1/e mode size of the fiber due to the high field intensity occurring at the corners of the metal wire, reflecting the importance of using suitable measures of plasmon mode size for a particular application, as pointed out by Oulton et al. [11].

Figure 1 shows the calculated propagation loss and coupling loss for gold wires with a square cross-section, with the side length of the square varying between 150 and 210 nm. Since the polymer layers are not infinitely thick, they provide an additional confinement for the plasmon mode. Calculations for infinitely wide dielectric therefore give weaker confinement and lower propagation loss values [7, 9]. The total thickness of the cladding in our simulations was varied between 12 and 40  $\mu\text{m}$ , with the wire being sandwiched halfway through. As expected, similar results are obtained for both polarizations in the symmetric wire case. It should be emphasized that the simulation only accounts for propagation loss due to the damping effect of the metal. A weakly bound mode with low damping will suffer larger bending losses as well as increased scattering losses due to imperfections in the metal wire (roughness) or polymer film.

While the propagation loss increases with the size of the wire cross-section, the coupling loss decreases, as the overlap with the fiber mode improves. As noted above, the finite-thickness cladding also provides additional confinement. For narrow wires, the increased confinement from a thinner cladding substantially decreases the coupling loss while causing only a modest increase in propagation loss for short devices. In order to minimize the insertion loss for a given device length, a compromise must therefore be reached, depending on the geometry of the particular geometry.

In order to determine geometric tolerances for realizing polarization-independent waveguides, we considered the case of slightly asymmetrical cross-sections: a rectangle with the height of 180 nm and widths ranging from 160 to 200 nm (with the same rounded corners as in case of the symmetrical wires). The results of the simulation are shown in Fig. 2. It is evident that a 5% asymmetry ( $(|h-w|/h)$ ) can result in substantial polarization-dependent loss. The coupling and propagation loss values, however, are affected differently, and the variation is also influenced by the cladding thickness. Again, the correct compromise based on the actual device geometry can be used to improve the tolerance to fabrication errors.

In order to determine the minimum insertion loss for straight-waveguide sections of different length, we calculated propagation losses and fiber-to-fiber coupling losses for different cladding thicknesses as shown in Fig. 3, right panel. Taking the cladding thickness that gives a minimum insertion loss for short (0.5–1 mm) devices, we also calculated the

effect of reducing the width of the cladding layer in the horizontal direction, as shown in Fig. 3, left panel. This results in a minimum insertion loss close to 1.4 dB for the 0.5 mm device length. We have previously demonstrated short (1–2 mm) variable optical attenuator (VOA) devices with high extinction ratio based on electrically heated straight plasmonic nanowire waveguides [12] and propose that such devices can be made even shorter in order to realize insertion losses of around 1–2 dB. Such compact VOA devices could, e.g., be integrated within a polymer PLC platform.

Finally, we have noted experimentally that metal deposition of nanostructures with high aspect ratios does not result in vertical sidewalls. We therefore investigated the effect of a trapezoidal wire shape on the calculated polarization dependence of the wires while keeping the cross-sectional area constant. For modest side wall angles (up to 6°), the difference in propagation loss for the two linear polarizations remains small (<0.1 dB/mm) and should not contribute significantly to PDL in short samples.

In summary, we have modeled plasmonic nanowire waveguides consisting of gold nanowires embedded in a dielectric cladding and investigated the effects of the shape of the wire cross-section and the cladding thickness on the propagation and coupling loss. The critical dimensions and geometric tolerances required for realizing zero-PDL long-range plasmonic waveguides are within the capabilities of current lithographic techniques. Compact (sub-millimeter) components utilizing the properties of the metallic waveguide could therefore be considered for integration with conventional dielectric waveguide platforms operating at telecom wavelengths.

**Acknowledgments** The project was supported by the Icelandic Research Fund, the Eimskip Research Fund at the University of Iceland.

## References

1. Ebbesen TW, Genet C, Bozhevolnyi SI (2008) *Phys Today* 61:44
2. Hoa XD, Kirk AG, Tabrizian M (2007) *Biosens Bioelectron* 23:151
3. Berini P (1999) *Opt Lett* 24:1011
4. Nikolajsen T, Leosson K, Salakhutdinov I, Bozhevolnyi SI (2003) *Appl Phys Lett* 82:668
5. Boltasseva A, Nikolajsen T, Leosson K, Kjaer K, Larsen MS, Bozhevolnyi SI (2005) *J Lightwave Technol* 23:413
6. Degiron A, Berini P, Smith DR (2008) *Opt Photon News* 19:29
7. Berini P (2004) US Patent number 6,741,782
8. Leosson K, Nikolajsen T, Boltasseva A, Bozhevolnyi SI (2006) *Opt Express* 14:314
9. Jung J, Søndergaard T, Bozhevolnyi SI (2007) *Phys Rev B* 76:035434
10. Johnson PB, Christy RW (1972) *Phys Rev B* 6:4370
11. Oulton RF, Bartal G, Pile DFP, Zhang X (2008) *New J Phys* 10:105018
12. Leosson K, Rosesnzweig T, Hermannsson PG, Boltasseva A (2008) *Opt Express* 16:15546